

# Synthesis, Characterization, and Photophysical Properties of Some Heterodimetallic Bisporphyrins of Ytterbium and Transition Metals – Enhancement and Lifetime Extension of Yb<sup>3+</sup> Emission by Transition-Metal Porphyrin Sensitization

Feng-Lei Jiang,<sup>[a,b]</sup> Wai-Kwok Wong,<sup>\*,[b,c]</sup> Xun-Jin Zhu,<sup>[b]</sup> Gui-Jiang Zhou,<sup>[b]</sup> Wai-Yeung Wong,<sup>[b,c]</sup> Po-Lam Wu,<sup>[c,d]</sup> Hoi-Lam Tam,<sup>[c,d]</sup> Kok-Wai Cheah,<sup>[c,d]</sup> Cheng Ye,<sup>[e]</sup> and Yi Liu<sup>\*,[a]</sup>

**Keywords:** Lanthanides / Optical limiting / Photoluminescence / Porphyrins / Transition metals

A series of d-f heterodimetallic bisporphyrin complexes (**YbZn**, **YbPd**, and **YbPt**), in which a Yb<sup>III</sup> porphyrinate moiety is linked to a transition-metal porphyrinate moiety by a flexible three-carbon chain, were synthesized. They were fully characterized by high-resolution mass spectrometry, <sup>1</sup>H and <sup>31</sup>P NMR spectroscopy, electronic absorption, and fluorescence methods. Variable-temperature near-infrared photoluminescence studies showed that the transition-metal porphyrinate moiety would enhance the ytterbium(III) emission centered at about 998 nm and extend its emission life-

time. **YbPd** and **YbPt** showed large two-photon absorption cross-section values because of the interaction between the porphyrin units, which caused a loss of centrosymmetry. Optical limiting investigation demonstrated that [Yb(TPP)-(L<sub>OMe</sub>)] and **YbPt** have comparable performance to C<sub>60</sub> by virtue of their heavy-metal effect. Our results indicate that these bisporphyrin dimetallic complexes will find valuable applications in the field of nonlinear optics.

(© Wiley-VCH Verlag GmbH & Co. KGaA, 69451 Weinheim, Germany, 2007)

## Introduction

In the late 1970s, bisporphyrins with four linkages each on the *meso* position<sup>[1a]</sup> and  $\beta$  position<sup>[1b]</sup> were reported. Later on, bisporphyrins and their metal complexes were synthesized to study the photoinduced energy transfer from porphyrin to O<sub>2</sub>.<sup>[2]</sup> Bisporphyrins are basically divided into two classes by virtue of their conformations: cofacial (mostly linked on the *ortho* position of the *meso*-phenyl group of porphyrin macrocycles) and linear (mostly linked on the *para* position of the *meso*-phenyl group of porphyrin macrocycles). Other than the linkage at the *meso*-phenyl

group, there are bisporphyrins with linkages at the  $\beta$  position of the pyrrole unit as well.<sup>[3]</sup> Bisporphyrins with various kinds of linkages and different central metal ions have attracted much attention because of their potential application in host–guest chemistry,<sup>[4]</sup> chemical sensing,<sup>[5]</sup> supramolecular chirogenesis,<sup>[6]</sup> catalytic photooxidation,<sup>[7]</sup> molecular switches,<sup>[8]</sup> photoinduced energy transfer,<sup>[9]</sup> two-photon absorption,<sup>[10]</sup> etc. Linear bisporphyrins were mainly investigated on the energy transfer from one porphyrin unit to the other one by varying the rigid linkages, such as the phenylene and alkyne units.<sup>[11]</sup>

Trivalent lanthanide ions continue to attract considerable interest because of their unique optical properties such as line-like emission bands and relatively long luminescence lifetimes.<sup>[12]</sup> However, while it was recently reported that Sm<sup>2+</sup> complexes can be directly excited because the transitions are allowed,<sup>[13a]</sup> it is generally difficult to excite lanthanide ions directly because of the forbidden nature of their electronic transitions.<sup>[13]</sup> In order to overcome this problem, lanthanide ions are usually excited by the energy transferred from organic chromophores, which can encapsulate the lanthanide ions. Porphyrin can act as an antenna for photoluminescence (PL) in light of its highly conjugated system, which absorbs strongly in the UV/Vis region. Ytterbium(III) complexes, which emit in the near-infrared (NIR) region centered at about 998 nm, where biological tissues and fluids are relatively transparent, are promising probes

[a] College of Chemistry and Molecular Sciences, Wuhan University, 430072 Wuhan, P. R. China  
Fax: +86-27-68754067  
E-mail: prof.liuyi@263.net

[b] Department of Chemistry, Hong Kong Baptist University, Waterloo Road, Hong Kong, P. R. China  
Fax: +852-3411-7348  
E-mail: wkwong@hkbu.edu.hk

[c] Centre for Advanced Luminescence Materials, Hong Kong Baptist University, Waterloo Road, Hong Kong, P. R. China

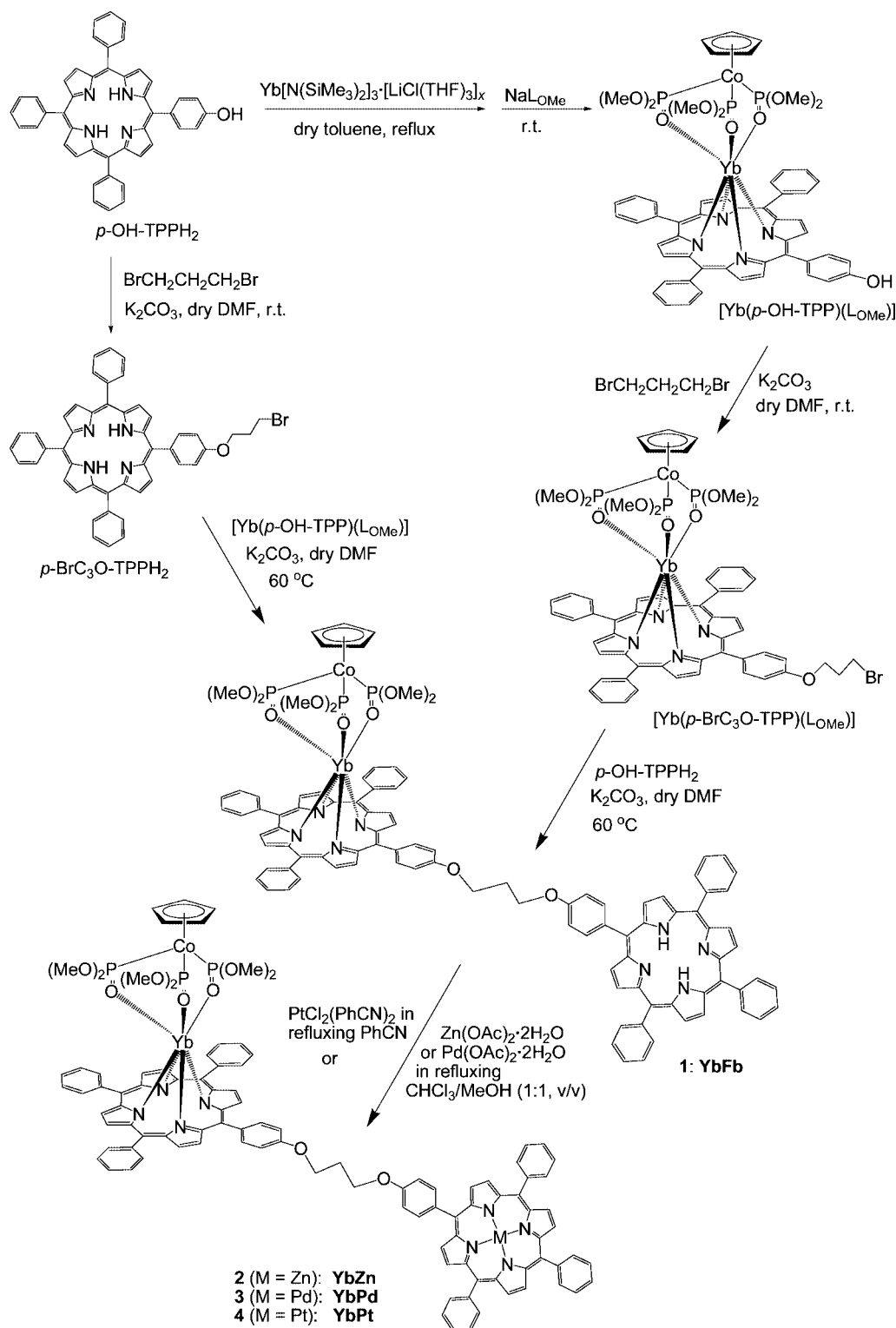
[d] Department of Physics, Hong Kong Baptist University, Waterloo Road, Hong Kong, P. R. China

[e] Center for Molecular Science, Institute of Chemistry, Chinese Academy of Sciences, 10080 Beijing, P. R. China

Supporting information for this article is available on the WWW under <http://www.eurjic.org> or from the author.

for fluoroimmunoassays. We have shown that porphyrinato ligands could act as antennae and sensitize NIR emission of  $\text{Nd}^{3+}$ ,  $\text{Er}^{3+}$ , and  $\text{Yb}^{3+}$  ions.<sup>[14]</sup> Recently, there has been considerable interest in extending the lifetimes of  $\text{Nd}^{\text{III}}$ ,  $\text{Er}^{\text{III}}$ , and  $\text{Yb}^{\text{III}}$ . Transition-metal ions with long lifetimes, such as  $\text{Cr}^{\text{III}}$ ,  $\text{Ru}^{\text{II}}$ , and  $\text{Pt}^{\text{II}}$ , were inserted into d-f heterodi-

metallic complexes and found to serve as sensitizers for lanthanide ions.<sup>[15–17]</sup> The best result of lifetime extension was observed for the  $\text{CrLn}$  ( $\text{Ln} = \text{Nd}, \text{Yb}$ ) complex,<sup>[15]</sup> which showed that  $\text{Cr}^{\text{III}} \rightarrow \text{Ln}^{\text{III}}$  intramolecular energy transfer could extend the lifetimes of lanthanide ions from the microsecond to millisecond timescale at 10 K. However, the



Scheme 1. Preparation of the dyads **YbFb**, **YbZn**, **YbPd**, and **YbPt**.

ligands only absorbed light in the high-energy region at 247 and 334 nm. To this end, we want to develop a strategy to extend the lanthanide lifetime by using sensitizers that absorb strongly in the UV/Vis region, such as metalloporphyrins of transition metals. To the best of our knowledge, there is no report in the literature on the synthesis of bisporphyrin complexes containing a lanthanide and a d-block transition metal. Herein, we report the synthesis, and photophysical and optical limiting properties of several bisporphyrin complexes, in which a Yb<sup>III</sup> porphyrinate moiety is linked to a transition-metal porphyrinate moiety by a flexible three-carbon chain.

## Results and Discussion

### Synthesis

Ytterbium(III) bisporphyrinate complexes **YbFb** (**1**), **YbZn** (**2**), **YbPd** (**3**), and **YbPt** (**4**) were prepared as shown in Scheme 1. When 5-(*p*-hydroxyphenyl)-10,15,20-triphenylporphyrin (*p*-OH-TPPH<sub>2</sub>) was treated with excess Yb[N(SiMe<sub>3</sub>)<sub>2</sub>]<sub>3</sub>·[LiCl(THF)]<sub>3</sub> under nitrogen in refluxing toluene for 12 h followed by the addition of excess Na{( $\eta^5$ -C<sub>5</sub>H<sub>5</sub>)Co[P(=O)(OMe)<sub>2</sub>]}<sub>3</sub> (NaL<sub>OMe</sub>) to the reaction mixture at room temperature (room temp.), workup gave purple air-stable crystals of [Yb(*p*-OH-TPP)(L<sub>OMe</sub>)] in 84% yield. The complex [Yb(*p*-OH-TPP)(L<sub>OMe</sub>)] was quite stable towards moisture and could be purified by column chromatography on silica gel. In the presence of K<sub>2</sub>CO<sub>3</sub>, reaction of *p*-OH-TPPH<sub>2</sub> with excess 1,3-dibromopropane in dry DMF under nitrogen at room temp. overnight gave 5-[*p*-(3-bromopropoxy)phenyl]-10,15,20-triphenylporphyrin (*p*-BrC<sub>3</sub>O-TPPH<sub>2</sub>) in 94% yield. The interaction of [Yb(*p*-OH-TPP)(L<sub>OMe</sub>)] with *p*-BrC<sub>3</sub>O-TPPH<sub>2</sub>, in the presence of

K<sub>2</sub>CO<sub>3</sub> in dry DMF at 60 °C overnight, gave the porphyrin complex **YbFb** (**1**), in which a porphyrin free base is appended to the Yb<sup>III</sup> porphyrinate complex by a flexible linkage, -OCH<sub>2</sub>CH<sub>2</sub>CH<sub>2</sub>O-, in 58% yield. **YbFb** could also be prepared by the reaction of *p*-OH-H<sub>2</sub>TPP with [Yb(*p*-BrC<sub>3</sub>O-TPP)(L<sub>OMe</sub>)], which was synthesized by the reaction of [Yb(*p*-OH-TPP)(L<sub>OMe</sub>)] with 1,3-dibromopropane in the presence of K<sub>2</sub>CO<sub>3</sub>. All the above porphyrin free bases and Yb porphyrinate complexes were fully characterized by <sup>1</sup>H and <sup>31</sup>P (if applicable) NMR, MS, and UV/Vis spectroscopy. The solid-state structure of [Yb(*p*-BrC<sub>3</sub>O-TPP)(L<sub>OMe</sub>)] (Figure 1), ascertained by X-ray crystallography, is very similar to that of [Yb(TMPP)(L<sub>OMe</sub>)].<sup>[14c]</sup> Crystal structure analysis revealed that the Yb ion is seven-coordinate, surrounded by four N atoms of the porphyrinate dianion and three O atoms of the three phosphito groups. The Yb–N and Yb–O distances are in the ranges 2.343(6)–2.367(5) and 2.260(7)–2.281(7) Å, respectively. The bond lengths and bond angles are almost the same as those in [Yb(TMPP)(L<sub>OMe</sub>)].<sup>[14c]</sup>

When **YbFb** was treated with M(OAc)<sub>2</sub>·2H<sub>2</sub>O (M = Zn, Pd) in a refluxing CHCl<sub>3</sub>/MeOH (1:1, v/v) mixture for 24 h, **YbZn** (**2**) and **YbPd** (**3**) were obtained in 83% and 88% yields, respectively; and with PtCl<sub>2</sub>(PhCN)<sub>2</sub> in refluxing PhCN, **YbPt** (**4**) was obtained in 60% yield. Complexes **1–4** are thermally and air-stable and can be purified by column chromatography. The four bisporphyrins were fully characterized by mass spectrometry, <sup>1</sup>H and <sup>31</sup>P (if applicable) NMR, and UV/Vis spectroscopy. The MALDI-TOF mass spectra of complexes **1–4** exhibit the [M + 1]<sup>+</sup> peaks at *m/z* = 1924.4353, 1988.3409, 2028.3187, and 2117.3801, respectively, which deviate less than 5 ppm from the theoretical values of 1924.4363, 1988.3490, 2028.3251, and 2117.3859, respectively, and their isotopic distribution patterns match

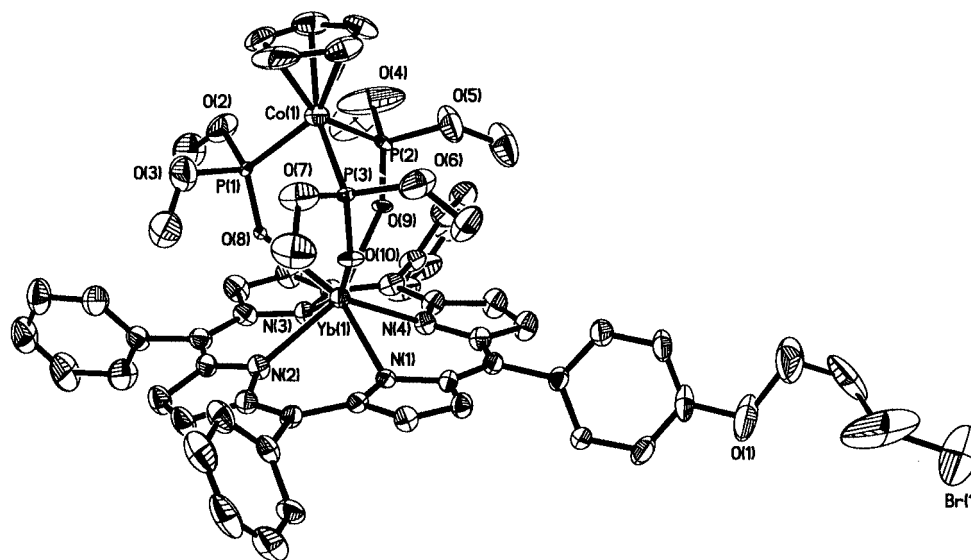


Figure 1. Perspective drawing of [Yb(*p*-BrC<sub>3</sub>O-TPP)(L<sub>OMe</sub>)]. Hydrogen atoms were omitted for clarity. Selected bond lengths [Å] and bond angles [°]: N(1)–Yb(1) 2.367(5), N(2)–Yb(1) 2.350(6), N(3)–Yb(1) 2.343(6), N(4)–Yb(1) 2.350(5), O(8)–Yb(1) 2.260(7), O(9)–Yb(1) 2.280(7), O(10)–Yb(1) 2.281(7); O(8)–Yb(1)–O(9) 76.4(3), O(8)–Yb(1)–O(10) 78.9(3), O(9)–Yb(1)–O(10) 80.7(3), N(3)–Yb(1)–N(2) 77.99(19), N(3)–Yb(1)–N(4) 75.51(19), N(2)–Yb(1)–N(4) 122.5(2), N(3)–Yb(1)–N(1) 121.9(2), N(2)–Yb(1)–N(1) 76.17(18), N(4)–Yb(1)–N(1) 76.23(17).

the theoretical distribution. The  $^1\text{H}$  NMR spectrum (in  $\text{CDCl}_3$ ) of **1** shows a singlet at  $\delta = -2.64$  ppm for the inner NH groups of the porphyrin free base moiety. This peak is absent in the  $^1\text{H}$  NMR spectra of dyads **2–4**, which indicates that the transition metals are coordinated to the four nitrogen atoms of the appended porphyrin free base. The  $^1\text{H}$  NMR spectra of the four dyads exhibit single peaks at  $\delta = -4.52$  ppm for the five cyclopentadienyl protons, quartets at  $\delta \approx 3.34$  ppm for the  $-\text{OCH}_2\text{CH}_2\text{CH}_2\text{O}-$  protons, and two triplets at  $\delta \approx 5.20$  and  $5.64$  ppm for the  $-\text{OCH}_2\text{CH}_2\text{CH}_2\text{O}-$  protons. The  $^{31}\text{P}\{^1\text{H}\}$  NMR spectra (vs. 85%  $\text{H}_3\text{PO}_4$ ) of **1–4** show single peaks at  $\delta = 69.2$ ,  $69.2$ ,  $69.2$ , and  $69.0$  ppm, respectively, for the phosphito groups of the anionic  $\text{LOMe}^-$  ligand.

### Photophysical Properties

The photophysical properties of the four dyads **1–4** have been examined and the data are summarized in Table 1. The absorption spectrum of each of the four dyads **1–4** is the sum of the absorption spectra of the two separate porphyrinate moieties,  $[\text{Yb}(\text{TPP})(\text{LOMe})]$  and  $[\text{M}(\text{TPP})]$  ( $\text{M} = \text{H}_2$ ,  $\text{Zn}$ ,  $\text{Pd}$  or  $\text{Pt}$ ). Figure 2 shows the absorption spectra of  $[\text{Yb}(\text{TPP})(\text{LOMe})]$ ,  $[\text{Pt}(\text{TPP})]$ , and **4** (**YbPt**) in toluene at room temp. The room-temperature solution electronic absorption, excitation, and emission spectra of **1–4** in the UV/Vis region are characteristic of intraligand transitions of normal porphyrinate complexes. The absorption bands (Soret and Q bands) and emission peaks in the visible region are typical of the intraligand  $\pi \rightarrow \pi^*$  transitions of the porphyrinato ligand. The visible emissions, which have a decay time ( $\tau$ ) of about 3.79–9.17 ns and quantum yields ( $\Phi_{\text{em}}$ ) of  $(1.1\text{--}9.1) \times 10^{-2}$ , can be assigned to the  $\text{S}_1 \rightarrow \text{S}_0$  ligand-centered singlet ( $^1\text{LC}$ ) fluorescence. The photoluminescence intensity of the four dyads strongly increases at 77 K and other than for **YbFb**, which exhibits no bathochromicity, the emission peaks of the dyads are redshifted by about 10 nm as compared with their emission bands at room

temp. Lifetime measurements at 77 K showed that unlike dyads **YbFb** and **YbZn**, which exhibit only  $^1\text{LC}$  fluorescence at 652 ( $\tau = 12.96$  ns) and 611 ( $\tau = 3.88$  ns) nm, respectively, dyads **YbPd** and **YbPt** also exhibit phosphorescence at 693 ( $\tau = 950$   $\mu\text{s}$ ) and 660 ( $\tau = 100$   $\mu\text{s}$ ) nm, which almost coincides with the ligand-centered triplet ( $^3\text{LC}$ ) emission of  $[\text{Pd}(\text{TPP})]$  and  $[\text{Pt}(\text{TPP})]$  complexes, respectively, and could be assigned to the  $^3\text{LC}$  emission of the  $[\text{M}(\text{TPP})]$  moiety of the dyads. Figure 3 shows the solution excitation and emission spectra of dyad **YbPd** and the  $[\text{Pd}(\text{TPP})]$  complex in the visible region at both room temp. and 77 K. The lowest  $^3\text{LC}$  state of the  $[\text{Yb}(\text{TPP})(\text{LOMe})]$  moiety of the dyads can be identified by measuring the emission spectrum and decay time of the  $[\text{Gd}(\text{TPP})(\text{LOMe})]$  complex.<sup>[18–21]</sup> This is possible because the metal-centered (MC) electronic levels of  $\text{Gd}^{3+}$  are known to be located at  $31000\text{ cm}^{-1}$ , typically well above the LC electronic levels of the aromatic ligands.<sup>[22]</sup> Therefore, ligand-to-metal energy transfer and the consequent MC luminescence cannot be observed. The time-resolved spectrum of the  $[\text{Gd}(\text{TPP})(\text{LOMe})]$  complex at 77 K shows that the LC long-lived phosphorescence is detected at 792 nm ( $\tau = 136$   $\mu\text{s}$ ).<sup>[23]</sup>

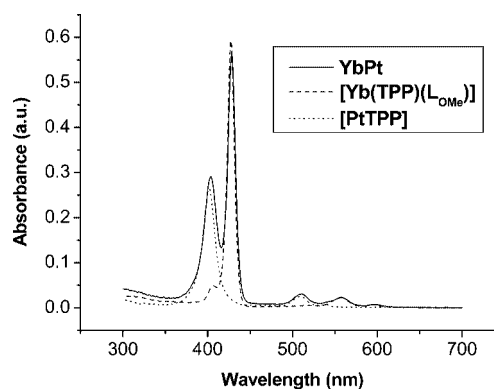


Figure 2. Absorption spectra of **YbPt**,  $[\text{Yb}(\text{TPP})(\text{LOMe})]$ , and  $[\text{Pt}(\text{TPP})]$ .

Table 1. Photophysical data of **YbFb**, **YbZn**, **YbPd**, and **YbPt** in toluene.<sup>[a]</sup>

Compound	Absorption $\lambda_{\text{max}}$ (log $\epsilon$ ) [nm ( $\text{dm}^3\text{mol}^{-1}\text{cm}^{-1}$ )]	Excitation $\lambda_{\text{exc}}$ [nm]	Emission at 298 K $\lambda_{\text{em}}$ [nm] ( $\tau$ , $\Phi_{\text{em}} \times 10^2$ ) <sup>[b–d]</sup>	Emission at 77 K $\lambda_{\text{em}}$ [nm] ( $\tau$ )
<b>YbFb</b>	428 (5.86), 517 (4.34), 556 (4.48) 595 (4.06), 646 (3.71)	419	652 (9.02 ns, 9.1), 717 998 (30 $\mu\text{s}$ )	652 (12.96 ns), 717 998 (30 $\mu\text{s}$ )
<b>YbZn</b>	427 (5.95), 557 (4.61), 595 (4.12)	422	601, 651 (3.79 ns, 1.1) 998 (30 $\mu\text{s}$ )	611 (3.88 ns), 670 998 (30 $\mu\text{s}$ )
<b>YbPd</b>	428 (5.81), 524 (4.51), 557 (4.43) 596 (3.92)	420	654 (9.17 ns, 1.6), 721 998 (40 $\mu\text{s}$ )	648, 693 (950 $\mu\text{s}$ ), 772 998 (40 $\mu\text{s}$ )
<b>YbPt</b>	403 (5.46), 428 (5.75), 511 (4.49) 558 (4.36), 596 (3.88)	420	652 (8.72 ns, 2.0), 716 998 (30 $\mu\text{s}$ )	660 (100 $\mu\text{s}$ ), 726 998 (70 $\mu\text{s}$ )
$[\text{Yb}(\text{TPP})(\text{LOMe})]$	428 (5.79), 558 (4.40), 597 (3.85)	419	652 (6.93 ns), 718 998 (30 $\mu\text{s}$ )	652 (9.15 ns), 718 998 (30 $\mu\text{s}$ )
$[\text{Gd}(\text{TPP})(\text{LOMe})]$	428 (5.86), 559 (4.35), 597 (3.76)	420	656 (9.92 ns), 720	650 (12.71 ns), 792 (136 $\mu\text{s}$ )
$[\text{Pd}(\text{TPP})]$	416, 524	420	610, 652, 715	698 (1340 $\mu\text{s}$ )
$[\text{Pt}(\text{TPP})]$	402, 509, 540	403	662	660 (120 $\mu\text{s}$ )

[a] Measurements were carried out at a concentration of  $1 \times 10^{-6}$  M in toluene. [b] The quantum yield standard used in this study was tetraphenylporphyrin ( $\text{H}_2\text{TPP}$ ) in anhydrous benzene in air ( $\Phi_{\text{F}} = 0.11$  at 298 K). Quantum yields were calculated using standard methods. [c] Near-infrared (NIR) photoluminescence measurements were carried out in toluene at a concentration of  $1 \times 10^{-6}$  M excited at 514 nm. [d] The wavelength of the laser for lifetime measurement was 337 nm.

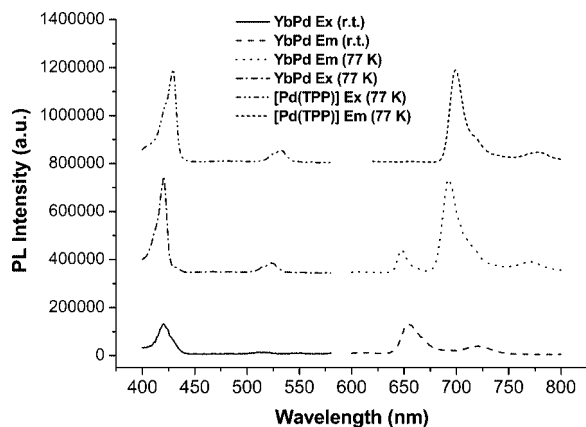


Figure 3. Excitation and emission spectra of **YbPd** and **[Pd(TPP)]** at 77 K and room temperature.

Other than the visible emission, dyads **1–4** also exhibit  $\text{Yb}^{3+}$  ion emission in the NIR region. The emissions at 998 nm can be assigned to the  $^2\text{F}_{5/2} \rightarrow ^2\text{F}_{7/2}$  transition of  $\text{Yb}^{3+}$ . These NIR emissions are very similar to those reported for  $\text{Yb}^{\text{III}}$  monoporphyrinate complexes, and the lifetime values are in good agreement with the literature values.<sup>[24,25]</sup> The  $\text{Yb}^{3+}$  luminescence lifetimes at room temp. lie within 30–40  $\mu\text{s}$  for the four dyads and are much longer than the lifetime of the porphyrinate emission. Figure 4 shows the visible and NIR emission and the excitation spectra of **YbPd** in toluene. The excitation spectrum of **YbPd** monitored at 998 nm is identical to that monitored at 654 nm, and its excitation bands at 526, 560, and 602 nm almost coincide with its visible absorption bands at 524, 557, and 596 nm. This clearly shows that both the visible and NIR emissions originate from the  $\pi \rightarrow \pi^*$  transitions of the porphyrinate antenna, and excitation of porphyrin is the photophysical pathway leading to the observable NIR luminescence. A comparison of the NIR luminescence intensity of the dyads with that of the  $[\text{Yb}(\text{TPP})(\text{L}_{\text{OMe}})]$  complex at room temp. shows that the relative intensity increases in the order of  $[\text{Yb}(\text{TPP})(\text{L}_{\text{OMe}})]$  (1.0) < **YbZn** (1.8) < **YbPd** (4.0) < **YbPt** (5.0) (Figure 5). This suggests that

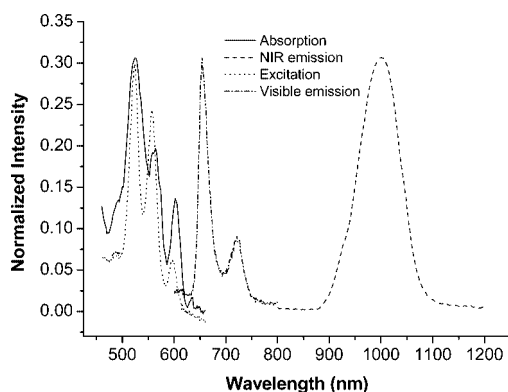


Figure 4. Room-temperature absorption, NIR emission (excited at 514 nm) and excitation (monitored at 998 nm) spectra of **YbPd** in toluene.

the  $[\text{M}(\text{TPP})]$  ( $\text{M} = \text{Zn}, \text{Pd}$  and  $\text{Pt}$ ) moiety, which contributes to the enhancement of NIR emission, transfers its energy to the  $\text{Yb}^{3+}$  ion. Fluorescence studies at room temp. further support the above donor-acceptor-based hypothesis. The visible fluorescence intensity of the **YbPd** dyad is much weaker than that of the **[Pd(TPP)]** complex (Figure 6). This indicates that the **[Pd(TPP)]** moiety (donor) of the **YbPd** dyad is quenched by the  $[\text{Yb}(\text{TPP})(\text{L}_{\text{OMe}})]$  moiety, probably by the transfer of the  $^1\text{LC}$  energy to the  $\text{Yb}^{3+}$  ion center (acceptor).

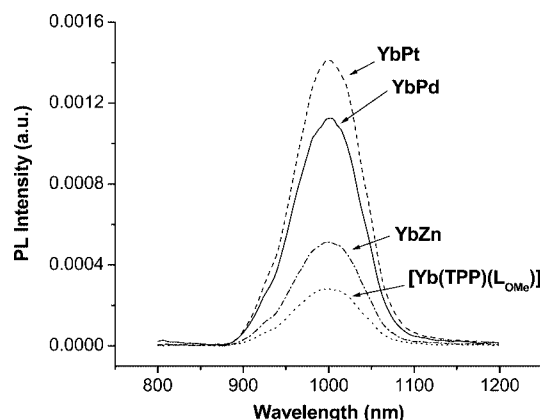


Figure 5. Near-infrared photoluminescence spectra excited at 514 nm at the same concentration in toluene.

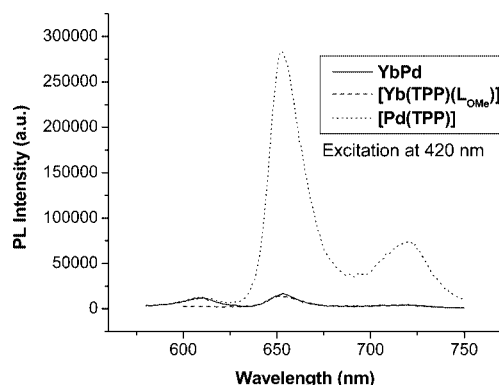


Figure 6. Emission spectra of **YbPd**,  $[\text{Yb}(\text{TPP})(\text{L}_{\text{OMe}})]$ , and **[Pd(TPP)]** at the same concentration at room temperature.

Optical absorption of the  $^1\text{M}(\text{TPP})$  unit leads to an  $\text{S}_0 \rightarrow \text{S}_1$  transition to the singlet excited state  $^1\text{M}(\text{TPP})^*$ , followed by a fluorescent emission or intersystem crossing to the triplet excited state  $^3\text{M}(\text{TPP})^*$ , which results in the phosphorescent emission and nonradiative deactivation with rate constants  $k_{\text{T}}$  and  $k_{\text{nr}}$  respectively. The energy of the  $^3\text{M}(\text{TPP})^*$  excited state can be transferred to  $(\text{Yb}^{3+})^*$  with rate constant  $k_{\text{ET}}$  so that the  $\text{Yb}^{\text{III}}$  NIR emission is enhanced and the lifetime extended (Figure 7). At 77 K, the  $\text{Yb}^{3+}$  luminescence lifetime of dyads **YbFb** and **YbZn** remains unchanged (30  $\mu\text{s}$ ) and is the same as that of  $[\text{Yb}(\text{TPP})(\text{L}_{\text{OMe}})]$ , whereas that of **YbPd** and **YbPt** is extended from 30 to 40 and 70  $\mu\text{s}$ , respectively. This may be



due to the presence of a very intense, long-lived  $^3\text{M}(\text{TPP})^*$  state in **YbPd** ( $\lambda = 693 \text{ nm}$ ,  $\tau = 950 \mu\text{s}$ ) and **YbPt** ( $\lambda = 660 \text{ nm}$ ,  $\tau = 100 \mu\text{s}$ ), which sensitizes and prolongs the lifetime of the  $\text{Yb}^{3+}$  luminescence. Such a long-lived  $^3\text{M}(\text{TPP})^*$  state is absent in **YbFb** and **YbZn**. The better extension of the  $\text{Yb}^{\text{III}}$  lifetime of **YbPt** than **YbPd** clearly shows that the efficiency of energy transfer by the triplet excited state is better in the former than in the latter.

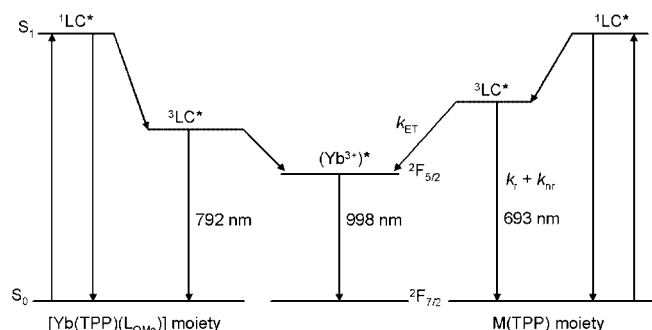


Figure 7. Scheme for the energy transfer from the transition-metal porphyrin unit {[Pd(TPP)] for example} to the Yb porphyrin unit (LC = ligand center).  $k_{\text{ET}}$  is the rate constant for energy transfer;  $k_r$  is the rate constant for radiative deactivation;  $k_{\text{nr}}$  is the rate constant for nonradiative deactivation.  $k_r + k_{\text{nr}} = \tau_0^{-1}$  and  $k_r + k_{\text{nr}} + k_{\text{ET}} = \tau^{-1}$ .

$\text{H}_2\text{TPP}$  and  $[\text{Zn}(\text{TPP})]$  are strongly fluorescent while  $[\text{Pd}(\text{TPP})]$  and  $[\text{Pt}(\text{TPP})]$  are strongly phosphorescent.<sup>[26]</sup> Brookfield et al.<sup>[27]</sup> investigated the energy transfer in Zn-metal-free porphyrin dimers and found that the Zn porphyrin unit transfers singlet-state excitation energy to the free-base porphyrin unit. For the bisporphyrins here, dipole–dipole energy transfer is the dominant mechanism. Here, the  $\text{Yb}^{\text{III}}$  ion is sensitized by two species: one is the porphyrin chromophore, which is coordinated to it; the other is the triplet excited state of the transition-metal porphyrinate unit, which enhances its NIR luminescence. Because the lifetimes of **YbPd** at 693 nm and **YbPt** at 660 nm at 77 K are mainly contributed by the triplet excited state  $^3\text{M}(\text{TPP})^*$  lifetimes of the  $[\text{Pd}(\text{TPP})]$  and  $[\text{Pt}(\text{TPP})]$  moiety, respectively, the rate constants for the energy transfer from the  $[\text{M}(\text{TPP})]$  chromophores to the  $\text{Yb}^{3+}$  ion,  $k_{\text{ET}}$ , can be calculated from Equation (1), where  $\tau$  and  $\tau_0$  are the lifetimes of

the donor-acceptor dyad (**YbPd** and **YbPt**) and the donor chromophore  $[\text{M}(\text{TPP})]$  ( $\text{M} = \text{Pd}$  and  $\text{Pt}$ ), respectively.

$$k_{\text{ET}} = \left( \frac{1}{\tau} - \frac{1}{\tau_0} \right) \quad (1)$$

As a result,  $k_{\text{ET}}$  for **YbPd** and **YbPt** is 306 and 1667  $\text{s}^{-1}$ , respectively. Comparing the  $k_{\text{ET}}$  values, triplet excited state energy transfer of **YbPt** is much faster than that of **YbPd**.

## Two-Photon Absorption

Porphyrin derivatives have attracted increasing attention because of their two-photon absorption (TPA) properties, which could be applied in many research fields, such as 3D microfabrication,<sup>[28]</sup> photodynamic therapy<sup>[29]</sup> and optical limiting.<sup>[30]</sup> The TPA efficacy, which is evaluated by the TPA cross-section value,  $\sigma^{(2)}$ , is defined as the excitation obtained by the simultaneous absorption of two photons at a longer wavelength followed by the emission at a shorter wavelength (Figure 8). Because of the low quantum yield of porphyrin, the nonlinear transmittance method was used to determine  $\sigma^{(2)}$ . In this paper,  $\sigma^{(2)}$  was measured at 800 nm with 100-fs pulses by an open-aperture Z-scan method. Porphyrin is supposed to be excited to the singlet excited state by simultaneously absorbing two photons at 800 nm. It can then emit photons at 650 nm or relax to the triplet excited state through intersystem crossing; thereafter energy could

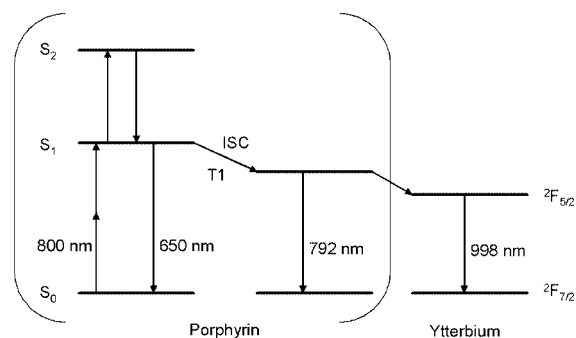


Figure 8. Scheme for the two-photon absorption of Yb porphyrinate complexes.

Table 2. TPA cross-section  $\sigma^{(2)}$  (GM) values.<sup>[a]</sup>

Compound	Concentration [mol L <sup>-1</sup> ]	$\beta$ [cm GW <sup>-1</sup> ]	Cross section $\sigma^{[b]}$ [GM]
YbFb	$2.5 \times 10^{-4}$	0.00061	101
YbZn	$2.5 \times 10^{-4}$	too weak	too weak
YbPd	$2.5 \times 10^{-4}$	0.00088	145
YbPt	$2.5 \times 10^{-4}$	0.00147	247
$[\text{Yb}(\text{TPP})(\text{L}_{\text{OMe}})]$	$2.5 \times 10^{-4}$	too weak	too weak
$\text{H}_2\text{TPP}$	$1 \times 10^{-3}$	0.00068	28
$[\text{Zn}(\text{TPP})]$	$1 \times 10^{-3}$	0.00036	15
$[\text{Pd}(\text{TPP})]$	$1 \times 10^{-3}$	0.00060	25
$[\text{Pt}(\text{TPP})]$	$1 \times 10^{-3}$	0.00067	28

[a] The TPA measurements were carried out at an excitation wavelength of 800 nm. [b] 1 GM =  $10^{-50} \text{ cm}^4 \cdot \text{s} \cdot \text{photon}^{-1}$ .

be transferred to the Yb<sup>III</sup> ion, which emits at 998 nm. While the  $\sigma^{(2)}$  value is wavelength-dependent, it is 28 GM for H<sub>2</sub>TPP at 800 nm in this work (cf. the reported value of 15 GM at 780 nm).<sup>[31]</sup> [Yb(TPP)(L<sub>OMe</sub>)] has a very low  $\sigma^{(2)}$  value, whereas the dyads YbFb, YbPd, and YbPt have four to eight times larger  $\sigma^{(2)}$  values than the corresponding transition-metal porphyrin [M(TPP)] monomers (Table 2).

### Optical Limiting Properties

Optical limiters are typically those dyes with nonlinear optical properties in which the light transmittance will decrease sharply under high light flux so that they can protect sensors from high optical power. Optical limiting (OL) effect can be explained by a mechanism known as reverse saturable absorption (RSA)<sup>[32]</sup> (see Supporting Information). Until now, indium tetra-*tert*-butylphthalocyanine chloride (InClPc) has been considered to be one of the best optical limiters.<sup>[33]</sup> Among many different kinds of OL materials, porphyrins continue to attract considerable attention because the structure-property relationships can be investigated easily through structural modification by changing the central metal center, ligand substituents etc. In general, porphyrins exhibit strong excited-state absorptions and long-lived triplet excited states.<sup>[30]</sup> In addition, they allow high transmission in the visible region because their ground-state absorptions are mainly confined to a few narrow regions (Soret and Q bands). Recently, the optical limiting properties of metalloporphyrins have been examined.<sup>[34]</sup> Herein, we studied the OL effect of our porphyrin dyads with the Z-scan technique<sup>[35]</sup> at 532 nm. The transmittances for YbPd, YbZn, YbPt, and [Yb(TPP)(L<sub>OMe</sub>)] decrease to 55%, 54%, 44%, and 40%, respectively, of their original linear transmission (Figure 9). The OL performance of [Yb(TPP)(L<sub>OMe</sub>)] and **4** is comparable to the benchmark material C<sub>60</sub>.

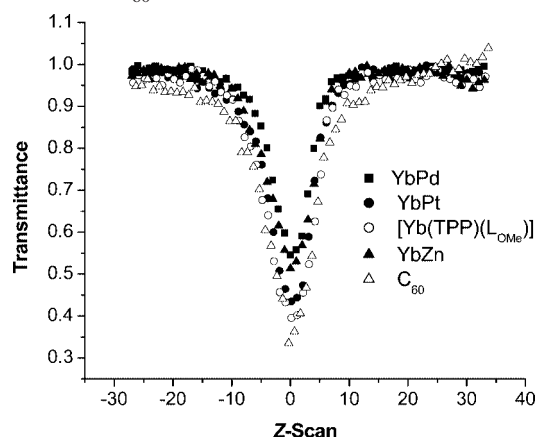


Figure 9. Open-aperture Z-scans at 532 nm for optical limiting measurements at a linear transmittance of 85%.

### Conclusions

We have prepared and characterized a series of d-f heterodimetallic bisporphyrin complexes, in which a Yb<sup>III</sup>

porphyrinate moiety was linked to a transition-metal porphyrinate moiety by a flexible three-carbon chain. Upon excitation at 514 nm, the four dyads gave NIR emission centered at 998 nm, with the emission intensity increasing in the order of YbZn < YbPd < YbPt. Photophysical studies showed that the transition-metal porphyrinate moiety sensitized NIR emission and enhanced the Yb<sup>III</sup> emission intensity and lifetime. Two-photon absorption (TPA) measurements at 800 nm showed that, except for YbZn, the bisporphyrins had much larger TPA cross-section values,  $\sigma^{(2)}$ , than those of [Yb(TPP)(L<sub>OMe</sub>)] and [M(TPP)] (M = H<sub>2</sub>, Zn, Pd, and Pt) complexes. The optical limiting (OP) measurements at 532 nm showed that the OL property was enhanced in the order of YbPd < YbZn < YbPt < [Yb(TPP)(L<sub>OMe</sub>)], and the OL performance of [Yb(TPP)(L<sub>OMe</sub>)] and YbPt is comparable to that of C<sub>60</sub>.

### Experimental Section

**General:** All reactions were carried out in dry nitrogen. Solvents were dried by standard procedures, distilled, and deaerated prior to use. All chemicals used were obtained from Aldrich Chemical Company. PtCl<sub>2</sub>(PhCN)<sub>2</sub>,<sup>[36]</sup> Yb[N(SiMe<sub>3</sub>)<sub>2</sub>]<sub>3</sub>·[LiCl(THF)<sub>3</sub>]<sub>x</sub>,<sup>[14d]</sup> and [Yb(TPP)(L<sub>OMe</sub>)]<sup>[14c]</sup> were prepared according to literature methods. Electronic absorption spectra in the UV/Vis region were recorded with a Varian Cary 100 UV/Vis spectrophotometer, steady-state visible fluorescence and PL excitation spectra were recorded with a Photon Technology International (PTI) Alphascan spectrofluorimeter, and visible decay spectra with a pico-N<sub>2</sub> laser system (PTI TimeMaster) using  $\lambda_{\text{exc}} = 337$  nm. NIR emission was detected by a liquid-nitrogen-cooled InSb IR detector (EG & G) with a preamplifier and recorded by a lock-in amplifier system as the third harmonics. Quantum yields of the visible emissions were computed according to the literature method<sup>[37]</sup> using tetraphenylporphyrin (H<sub>2</sub>TPP) as the reference standard ( $\Phi = 0.11$  at 419 nm in benzene in air). NMR spectra were recorded with a Varian Unity Inova 400 MHz spectrometer. <sup>1</sup>H NMR chemical shifts were referenced to internal deuterated chloroform and then recalculated to TMS ( $\delta = 0.00$  ppm) and those from the <sup>31</sup>P{<sup>1</sup>H} NMR spectra to external 85% H<sub>3</sub>PO<sub>4</sub>. High- and low-resolution mass spectra, reported as *m/z*, were obtained with an Autoflex Bruker MALDI-TOF system and a Finnigan MAT SSQ710 mass spectrometer, respectively. Elemental analyses carried out at the Department of Chemistry, Shanxi University, P. R. China.

**Two-Photon Absorption Measurement:** The two-photon absorption spectra were measured at 800 nm by using the open-aperture Z-scan method with 100-fs pulses with a peak power of 276 GW cm<sup>-2</sup> from an optical parametric amplifier operating at a 1-kHz repetition rate generated from a Ti:sapphire regenerative amplifier system. The laser beam was split into two parts by a beam splitter. One was monitored by a photodiode (D1) as the incident intensity reference, and the other (D2) was detected for the transmitted intensity. After passing through a lens with  $f = 20$  cm, the laser beam was focused and passed through a quartz cell. The position of the sample cell was moved along the laser-beam direction (*z* axis) by a computer-controlled translatable table, so the local power density within the sample cell would be changed under the constant incident intensity laser power level. Finally, the transmitted intensity from the sample cell was detected by the photodiode (D2). The photodiode (D2) was connected to the computer, so each transmitted intensity would be taken over 100 times iteration by the

computer. Assuming a Gaussian beam profile, the nonlinear absorption coefficient  $\beta$  can be obtained by curve fitting to the observed open-aperture traces with Equation (2), where  $\alpha_0$  is the linear absorption coefficient,  $l$  is the sample length, and  $z_0$  is the diffraction length of the incident beam.

$$T(z) = 1 - \frac{\beta I_0 (1 - e^{-\alpha_0 l})}{2\alpha_0 (1 + (z/z_0)^2)} \quad (2)$$

After obtaining the nonlinear absorption coefficient  $\beta$ , the TPA cross-section  $\sigma^{(2)}$  of one solute molecule (in units of  $1 \text{ GM} = 10^{-50} \text{ cm}^4 \text{ s photon}^{-1}$ ) can be determined by using Equation (3), where  $N_A$  is the Avogadro constant,  $d$  is the concentration of the TPA compound in solution,  $h$  is the Planck constant, and  $\nu$  is the frequency of the incident laser beam.

$$\sigma^{(2)} = \frac{1000 \beta h \nu}{N_A d} \quad (3)$$

**Optical Limiting Measurement:** The investigation of optical limiting properties was performed with a Q-switched Nd:YAG laser at the repetition of 10 Hz. The arrangement of the system is shown in the Supporting Information. The laser was frequency-doubled with an output wavelength of 532 nm with 10-ns pulse width for Gaussian mode by a frequency double crystal (FDC). Then the laser beam was split into two beams by a beam splitter (BS). One was used as the reference beam, which was received by a detector ( $D_1$ ), and the other was for the sample measurement and was focused with a lens ( $L_1, f = 20 \text{ cm}$ ). After transmitting the light beam through the sample (S), it entered another detector ( $D_2$ ). The sample to be measured was moved along a rail to change the incidence irradiance on it. The incident and transmitted energies were detected simultaneously by the two detectors  $D_1$  and  $D_2$  (LPE-1A) individually. The solution samples were measured in a 1-mm quartz cell.

#### Preparation of Porphyrin Free Bases

**5-(*p*-Hydroxyphenyl)-10,15,20-triphenylporphyrin (*p*-OH-TPPH<sub>2</sub>):** This compound was prepared according to a modified literature method.<sup>[14b]</sup> A solution of benzaldehyde (18.29 mL, 180 mmol) and *p*-hydroxybenzaldehyde (7.32 g, 60 mmol) in propionic acid (700 mL) was heated to 130 °C. Then freshly distilled pyrrole (16.65 mL, 240 mmol) in propionic acid (50 mL) was added slowly to the solution over a period of 0.5 h. The reaction mixture was heated to reflux for another 0.5 h and then cooled to room temp. Then the volume of the reaction mixture was reduced to about half of its original volume under reduced pressure, and methanol (300 mL) was added to the concentrated solution. The resultant solution was kept in a refrigerator overnight. Filtration gave about 4.5 g of crude product, which was redissolved in a minimum amount of chloroform and chromatographed on a silica gel column with dichloromethane as eluent. The second band gave the desired *p*-OH-TPPH<sub>2</sub>. Yield: 1.9 g (5%). FAB-MS: 631 [ $M + H$ ]<sup>+</sup>. <sup>1</sup>H NMR (CDCl<sub>3</sub>):  $\delta = -2.78$  (s, 2 H), 4.14 (s, 1 H), 7.19 (m, 2 H), 7.74 (m, 9 H), 8.05 (m, 2 H), 8.21 (m, 6 H), 8.85 (m, 8 H) ppm. UV/Vis (toluene):  $\lambda_{\text{max}}$  (log  $\epsilon$ ) = 419 (5.48), 515 (4.20), 550 (3.88), 592 (3.64), 651 (3.71 dm<sup>3</sup> mol<sup>-1</sup> cm<sup>-1</sup>) nm.

**5-[*p*-(3-Bromopropoxy)phenyl]-10,15,20-triphenylporphyrin (*p*-BrC<sub>3</sub>O-TPPH<sub>2</sub>):** This compound was prepared according to a modified literature method.<sup>[14b]</sup> 1,3-Dibromopropane (2 mL, 800  $\mu\text{L}$ , 7.9 mmol) was added to a suspension of *p*-OH-TPPH<sub>2</sub> (0.50 g, 0.8 mmol) and anhydrous K<sub>2</sub>CO<sub>3</sub> in dry DMF (20 mL).

The mixture was stirred at room temp., and the progress of the reaction was monitored by TLC. After 24 h, dichloromethane (20 mL) was added to the reaction mixture, which was then washed with water (6  $\times$  20 mL) until all of the DMF and potassium carbonate were removed. The organic phase was dried with sodium sulfate, filtered and the solvents were evaporated to dryness in vacuo. The residue was redissolved in a chloroform/hexane mixture (1:1, v/v) and chromatographed on a silica gel column using chloroform/hexane (5:1, v/v) as eluent. The first band gave the product *p*-BrC<sub>3</sub>O-TPPH<sub>2</sub>. Yield: 560 mg (94%). FAB-MS: 752 [ $M + H$ ]<sup>+</sup>. <sup>1</sup>H NMR (CDCl<sub>3</sub>):  $\delta = -2.77$  (s, 2 H), 2.50 (m, 2 H), 3.77 (q, 2 H), 4.38 (q, 2 H), 7.28 (m, 2 H), 7.74 (m, 9 H), 8.12 (m, 2 H), 8.21 (m, 6 H), 8.86 (m, 8 H) ppm. UV/Vis (toluene):  $\lambda_{\text{max}}$  (log  $\epsilon$ ) = 420 (5.43), 515 (4.07), 550 (3.74), 594 (3.50), 650 (3.44 dm<sup>3</sup> mol<sup>-1</sup> cm<sup>-1</sup>) nm.

#### Preparation of Yb Porphyrinate Complexes

**[Yb(*p*-OH-TPP)(L<sub>OMe</sub>)]:** This compound was prepared according to a modification of the literature method.<sup>[14c]</sup> After *p*-OH-TPPH<sub>2</sub> (518 mg, 0.82 mmol) had been treated with excess Yb[N(SiMe<sub>3</sub>)<sub>2</sub>]<sub>3</sub>·[LiCl(THF)<sub>3</sub>]<sub>x</sub> (0.16 mol L<sup>-1</sup>, 10 mL) under nitrogen in refluxing toluene for 12 h, the mixture was cooled down to room temp., followed by the addition of excess NaL<sub>OMe</sub>. The reaction mixture was concentrated under reduced pressure to remove toluene and purified by column chromatography on silica to give purple crystals of [Yb(*p*-OH-TPP)(L<sub>OMe</sub>)] after recrystallization. Yield: 863 mg (84%). MALDI-TOF MS: calcd. for [ $M^+$ ] 1253.1549, found 1253.1516. <sup>1</sup>H NMR (CDCl<sub>3</sub>):  $\delta = -4.62$  (s, 5 H), 6.98 (s, 18 H), 8.13 (s, 1 H), 8.57–8.76 (br., 8 H), 9.36–9.42 (br., 3 H), 9.93 (br., 1 H), 10.56 (br., 3 H), 15.29 (br., 8 H), 16.56 (br., 1 H), 16.85 (br., 3 H) ppm. <sup>31</sup>P{<sup>1</sup>H} NMR (CDCl<sub>3</sub>):  $\delta = 69.2$  ppm. UV/Vis (toluene):  $\lambda_{\text{max}}$  (log  $\epsilon$ ) = 429 (5.80), 558 (4.37), 599 (3.82 dm<sup>3</sup> mol<sup>-1</sup> cm<sup>-1</sup>) nm.

**[Yb(*p*-BrC<sub>3</sub>O-TPP)(L<sub>OMe</sub>)]:** [Yb(*p*-OH-TPP)(L<sub>OMe</sub>)] (100 mg, 0.08 mmol) was stirred in dry DMF (10 mL) in the presence of anhydrous potassium carbonate (300 mg) for 20 min, followed by addition of 10 equiv. of 1,3-dibromopropane. The reaction mixture was stirred overnight, and dichloromethane (20 mL) was then added. The mixture was washed with deionized water (3  $\times$  20 mL) until all the DMF was washed away. The solution was dried with anhydrous sodium sulfate, and the residue upon concentration was purified by column chromatography on silica with dichloromethane as eluent. The first band gave [Yb(*p*-BrC<sub>3</sub>O-TPP)(L<sub>OMe</sub>)]. Yield: 90 mg (82%). MALDI-TOF MS: calcd. for [ $M + H$ ]<sup>+</sup> 1374.1178, found 1374.1234. <sup>1</sup>H NMR (CDCl<sub>3</sub>):  $\delta = -4.54$  (s, 5 H), 3.25 (q, 2 H), 4.53 (t, 2 H), 5.38 (t, 2 H), 6.62 (s, 18 H), 8.38 (br., 1 H), 8.90–9.02 (br., 7 H), 9.64 (m, 3 H), 10.24 (br., 1 H), 10.80 (br., 3 H), 15.62 (br., 8 H), 16.87–17.18 (br., 4 H) ppm. <sup>31</sup>P{<sup>1</sup>H} NMR (CDCl<sub>3</sub>):  $\delta = 68.2$  ppm. UV/Vis (toluene):  $\lambda_{\text{max}}$  (log  $\epsilon$ ) = 429 (5.68), 558 (4.26), 598 (3.77 dm<sup>3</sup> mol<sup>-1</sup> cm<sup>-1</sup>) nm.

#### Preparation of Yb Bisporphyrin Complexes

**YbFb:** *p*-BrC<sub>3</sub>O-TPPH<sub>2</sub> (200 mg, 0.27 mmol) was added to a suspension of [Yb(*p*-OH-TPP)(L<sub>OMe</sub>)] (358 mg, 0.29 mmol) in dry DMF (10 mL) in the presence of anhydrous potassium carbonate. The resultant mixture was stirred at 60 °C overnight and cooled to room temp. Dichloromethane (10 mL) was added to the reaction mixture, which was then washed with water (6  $\times$  10 mL) until all of the DMF and potassium carbonate was removed. The organic phase was dried with sodium sulfate, filtered, and the solvents were evaporated to dryness in vacuo. The residue was redissolved in chloroform/hexane (1:1, v/v) and chromatographed on a silica gel column using chloroform/hexane (5:1, v/v) as eluent to give YbFb from the first band. Yield: 318 mg (58%). MALDI-TOF MS: calcd. for [ $M + H$ ]<sup>+</sup> 1924.4363, found 1924.4353. IR (KBr):  $\tilde{\nu} = 3446$  (s),



2939 (w), 1701 (w), 1652 (w), 1600 (w), 1511 (m), 1472 (m), 1438 (w), 1240 (m), 1175 (m), 1141 (s), 1035 (m), 1007 (m), 799 (s), 775 (m), 727 (s), 702 (m), 620 (w), 587 (m)  $\text{cm}^{-1}$ .  $^1\text{H}$  NMR ( $\text{CDCl}_3$ ):  $\delta$  = −4.52 (s, 5 H), −2.64 (s, 2 H), 3.34 (q, 2 H), 5.20 (t, 2 H), 5.64 (t, 2 H), 6.34 (s, 18 H), 7.20–7.83 (m, 11 H), 8.24–8.30 (m, 6 H), 8.47 (d, 2 H), 8.65–8.73 (br., 8 H), 8.89 (s, 4 H), 9.00 (d, 2 H), 9.19 (d, 2 H), 9.36 (br., 3 H), 10.15 (br., 1 H), 10.52 (br., 3 H), 15.22 (br., 8 H), 16.60–16.78 (br., 4 H) ppm.  $^{31}\text{P}\{^1\text{H}\}$  NMR ( $\text{CDCl}_3$ ):  $\delta$  = 69.2 ppm. **YbFb** could also be prepared by the reaction of  $[\text{Yb}(p\text{-BrC}_3\text{O-TPP})(\text{LOMe})]$  with  $p\text{-OH-TPPH}_2$ .  $[\text{Yb}(p\text{-BrC}_3\text{O-TPP})(\text{LOMe})]$  (100 mg, 0.073 mmol) was added to a suspension of  $p\text{-OH-TPPH}_2$  (70 mg, 0.11 mmol) in dry DMF (10 mL) in the presence of anhydrous potassium carbonate (300 mg). Then the resultant mixture was stirred at 60 °C overnight and cooled to room temp. Dichloromethane (10 mL) was added to the reaction mixture, which was then washed with water ( $6 \times 10$  mL) until all of the DMF and potassium carbonate were removed. The organic phase was dried with sodium sulfate, filtered, and the solvents were evaporated to dryness in vacuo. The residue was redissolved in chloroform/hexane (1:1, v/v) and chromatographed on a silica gel column using chloroform/hexane (5:1, v/v) as eluent to give **YbFb** from the first band. Yield: 84 mg (60%).  $\text{C}_{102}\text{H}_{85}\text{CoN}_8\text{O}_{11}\text{P}_3\text{Yb}\cdot\text{CHCl}_3\cdot 1.5\text{C}_7\text{H}_8\cdot 2\text{H}_2\text{O}$  (2217.32): calcd. C 61.48, H 4.64, N 5.05; found C 61.55, H 4.59, N 4.96.

**YbZn and YbPd:** **YbFb** (100 mg, 0.052 mmol) was treated with  $\text{Zn}(\text{OAc})_2$  hydrate (300 mg, 1.37 mmol) or  $\text{Pd}(\text{OAc})_2$  hydrate (550 mg, 2.45 mmol) in a refluxing solution mixture of chloroform/methanol (1:1, v/v) (20 mL) for 24 h. Then chloroform and methanol were removed in a rotary evaporator. The resulting solid was dissolved in chloroform and chromatographed on a silica gel column using chloroform/hexane (5:1, v/v) as eluent. The second band gave **YbZn** (86 mg, 83%) or **YbPd** (93 mg, 88%) in good yields. **YbZn:** MALDI-TOF MS: calcd. for  $[\text{M} + \text{H}]^+$  1988.3490, found 1988.3409. IR (KBr):  $\tilde{\nu}$  = 3449 (s), 2939 (w), 1711 (s), 1600 (w), 1513 (m), 1480 (m), 1436 (w), 1359 (m), 1333 (w), 1225 (m), 1174 (w), 1140 (s), 1097 (w), 1064 (w), 1034 (m), 997 (s), 837 (w), 797 (m), 752 (m), 725 (m), 702 (m), 654 (w), 620 (w), 588 (w), 531 (w)  $\text{cm}^{-1}$ .  $^1\text{H}$  NMR ( $\text{CDCl}_3$ ):  $\delta$  = −4.54 (s, 5 H), 3.34 (q, 2 H), 5.21 (t, 3 H), 5.62 (t, 3 H), 6.33 (s, 18 H), 7.76–7.83 (m, 11 H), 8.24–8.31 (m, 6 H), 8.48 (d, 2 H), 8.65–8.73 (br., 8 H), 8.98 (s, 4 H), 9.11 (d, 2 H), 9.30 (d, 2 H), 8.34–8.39 (br., 3 H), 10.13 (br., 1 H), 10.51 (br., 3 H), 15.23 (br., 8 H), 16.78 (br., 4 H) ppm.  $^{31}\text{P}\{^1\text{H}\}$  NMR ( $\text{CDCl}_3$ ):  $\delta$  = 69.2 ppm.  $\text{C}_{102}\text{H}_{83}\text{CoN}_8\text{O}_{11}\text{P}_3\text{YbZn}\cdot\text{CHCl}_3\cdot 1.5\text{C}_7\text{H}_8\cdot \text{H}_2\text{O}$  (2262.68): calcd. C 60.25, H 4.36, N 4.95; found C 60.30, H 4.41, N 4.93. **YbPd:** MALDI-TOF MS: calcd. for  $[\text{M} + \text{H}]^+$  2028.3251, found 2028.3187. IR (KBr):  $\tilde{\nu}$  = 3445 (s), 2939 (w), 1710 (s), 1599 (m), 1510 (m), 1474 (m), 1440 (m), 1354 (m), 1238 (m), 1140 (s), 1009 (s), 798 (m), 752 (m), 725 (m), 704 (m), 587 (m)  $\text{cm}^{-1}$ .  $^1\text{H}$  NMR ( $\text{CDCl}_3$ ):  $\delta$  = −4.54 (s, 5 H), 3.30 (q, 2 H), 5.14 (t, 2 H), 5.60 (t, 2 H), 6.34 (s, 18 H), 7.77 (m, 11 H), 8.23 (m, 6 H), 8.40 (d, 2 H), 8.73 (br., 8 H), 8.87 (s, 4 H), 8.97 (d, 2 H), 9.15 (d, 2 H), 9.37 (br., 3 H), 10.12 (br., 1 H), 10.52 (br., 3 H), 15.24 (br., 8 H), 16.79 (br., 4 H) ppm.  $^{31}\text{P}\{^1\text{H}\}$  NMR ( $\text{CDCl}_3$ ):  $\delta$  = 69.2 ppm.  $\text{C}_{102}\text{H}_{83}\text{CoN}_8\text{O}_{11}\text{P}_3\text{PdYb}\cdot\text{CHCl}_3\cdot \text{C}_7\text{H}_8\cdot \text{H}_2\text{O}$  (2257.64): calcd. C 58.52, H 4.20, N 4.96; found C 58.51, H 4.18, N 4.88.

**YbPt:** After **YbFb** (100 mg, 0.052 mmol) had been treated with  $\text{PtCl}_2(\text{PhCN})_2$  (125 mg, 0.26 mmol) in refluxing benzonitrile (5 mL) for 24 h, the solvent was removed under reduced pressure. The resulting solid was dissolved in a minimum amount of dichloromethane and chromatographed on a silica gel column using dichloromethane as eluent. The second band gave **YbPt** in 60% yield (66 mg). MALDI-TOF MS: calcd. for  $[\text{M} + \text{H}]^+$  2117.3859, found 2117.3801. IR (KBr):  $\tilde{\nu}$  = 3434 (s), 2925 (m), 1602 (m), 1510

(w), 1444 (w), 1359 (w), 1325 (w), 1240 (m), 1175 (m), 1142 (s), 1014 (s), 796 (m), 753 (m), 726 (m), 704 (m), 588 (m)  $\text{cm}^{-1}$ .  $^1\text{H}$  NMR ( $\text{CDCl}_3$ ):  $\delta$  = −4.53 (s, 5 H), 3.36 (q, 2 H), 5.22 (t, 2 H), 5.67 (t, 2 H), 6.35 (s, 18 H), 7.74–7.82 (m, 11 H), 8.21 (m, 6 H), 8.41 (d, 2 H), 8.55–8.75 (br., 8 H), 8.80 (s, 4 H), 8.91 (d, 2 H), 9.10 (d, 2 H), 9.38 (br., 3 H), 10.14 (br., 1 H), 10.52 (br., 3 H), 15.25 (br., 8 H), 16.81 (br., 4 H) ppm.  $^{31}\text{P}\{^1\text{H}\}$  NMR ( $\text{CDCl}_3$ ):  $\delta$  = 69.0 ppm.  $\text{C}_{102}\text{H}_{83}\text{CoN}_8\text{O}_{11}\text{P}_3\text{PtYb}\cdot\text{CHCl}_3\cdot 1.5\text{C}_7\text{H}_8$  (2374.36): calcd. C 57.41, H 4.08, N 4.72; found C 57.57, H 4.02, N 5.08.

**X-ray Crystallography:** Pertinent crystallographic data and other experimental details are summarized in Table 3. Crystals of  $[\text{Yb}(p\text{-BrC}_3\text{O-TPP})(\text{LOMe})]\cdot 2\text{CHCl}_3$  suitable for X-ray diffraction studies were grown by slow concentration of a chloroform/methanol solution of the complex in air. The crystals were wrapped in epoxy glue to prevent them from losing solvent, and mounted on a thin glass fiber. Intensity data were collected at 293 K with a Bruker Axs SMART 100 CCD area-detector diffractometer using graphite-monochromated  $\text{Mo-K}_\alpha$  radiation ( $\lambda$  = 0.71073 Å). The collected frames were processed with the software SAINT<sup>[38]</sup> and an absorption correction was applied (SADABS<sup>[39]</sup>) to the collected reflections. The space group of the crystal was determined from the systematic absences and Laue symmetry checks and confirmed by successful refinement of the structure. The structure was solved by direct methods (SHELXTL<sup>[40]</sup>) and refined against  $F^2$  by full-matrix least-squares analyses. All non-hydrogen atoms were refined anisotropically. Hydrogen atoms were generated in their idealized positions and allowed to ride on their respective parent carbon atoms. CCDC-635196 contains the supplementary crystallographic data for this paper. These data can be obtained free of charge from The Cambridge Crystallographic Data Centre via [www.ccdc.cam.ac.uk/data\\_request/cif](http://www.ccdc.cam.ac.uk/data_request/cif).

Table 3. Crystallographic data for  $[\text{Yb}(p\text{-BrC}_3\text{O-TPP})(\text{LOMe})]\cdot 2\text{CHCl}_3$ .

Empirical formula	$\text{C}_{60}\text{H}_{58}\text{BrCl}_6\text{CoN}_4\text{O}_{10}\text{P}_3\text{Yb}$
Formula mass	1612.59
Color and habit	purple block
Crystal size [mm]	$0.30 \times 0.25 \times 0.21$
Crystal system	monoclinic
Space group	$P2_1/c$
$a$ [Å]	13.2139(6)
$b$ [Å]	43.627(2)
$c$ [Å]	12.3255(6)
$\alpha$ [°]	90
$\beta$ [°]	109.3310(10)
$\gamma$ [°]	90
$V$ [Å <sup>3</sup> ]	6704.9(6)
$Z$	4
$D_{\text{calcd.}}$ [g cm <sup>−3</sup> ]	1.598
Absorption coefficient [mm <sup>−1</sup> ]	2.597
$F(000)$	3220
$\theta$ range [°]	1.87–25.00
Reflections collected	32118
Independent reflections	11531 ( $R_{\text{int}}$ = 0.0429)
Observed reflections [ $I > 2.0\sigma(I)$ ]	8698
Goodness of fit on $F^2$	1.098
Final $R$ indices [ $I > 2\sigma(I)$ ]	$R_1$ = 0.0785, $wR_2$ = 0.1807
$R$ indices (all data)	$R_1$ = 0.1063, $wR_2$ = 0.1955

**Supporting Information** (see footnote on the first page of this article):  $^1\text{H}$  NMR and COSY spectra of  $[\text{Yb}(\text{TPP})(\text{LOMe})]$ , the optical limiting (OL) mechanism and experimental setup for OL.

## Acknowledgments

We thank the Hong Kong Baptist University (Grant FRG/03-04/II-05), the Hong Kong Research Grants Council (Grant HKBU 2023/04P), the National Natural Science Foundation of China (30570015), and the Science Fund for Creative Research Group (No. 20621502 NSFC) for financial support.

- [1] a) N. E. Kagan, D. Mauzerall, R. B. Merrifield, *J. Am. Chem. Soc.* **1977**, *99*, 5484–5486; b) I. Kunihiro, *Chem. Lett.* **1977**, *6*, 641–644.
- [2] a) P. Maillard, P. Krausz, C. Giannotti, *J. Organomet. Chem.* **1980**, *197*, 285–290; b) P. Maillard, S. Gaspard, P. Krausz, C. Giannotti, *J. Organomet. Chem.* **1981**, *212*, 185–191.
- [3] L. Jiao, B. H. Courtney, F. R. Fronczek, K. M. Smith, *Tetrahedron Lett.* **2006**, *47*, 501–504.
- [4] a) K. Wada, T. Mizutani, H. Matsuoka, S. Kitagawa, *Chem. Eur. J.* **2003**, *9*, 2368–2380; b) T. Mizutani, K. Wada, S. Kitagawa, *Chem. Commun.* **2002**, 1626–1627; c) T. Mizutani, K. Wada, S. Kitagawa, *J. Am. Chem. Soc.* **2001**, *123*, 6459–6460.
- [5] X.-B. Zhang, C.-C. Guo, Z.-Z. Li, G.-L. Shen, R.-Q. Yu, *Anal. Chem.* **2002**, *74*, 821–825.
- [6] V. V. Borovkov, G. A. Hembury, Y. Inoue, *Acc. Chem. Res.* **2004**, *37*, 449–459.
- [7] a) B. J. Pistorio, C. J. Chang, D. G. Nocera, *J. Am. Chem. Soc.* **2002**, *124*, 7884–7885; b) J. Rosenthal, B. J. Pistorio, L. L. Chng, D. G. Nocera, *J. Org. Chem.* **2005**, *70*, 1885–1888.
- [8] a) G. Pognon, C. Boudon, K. J. Schenk, M. Bonin, B. Bach, J. Weiss, *J. Am. Chem. Soc.* **2006**, *128*, 3488–3489; b) Y. Tomohiro, A. Satake, Y. Kobuke, *J. Org. Chem.* **2001**, *66*, 8442–8446.
- [9] S. Faure, C. Stern, R. Guillard, P. D. Harvey, *J. Am. Chem. Soc.* **2004**, *126*, 1253–1261.
- [10] K. Ogawa, A. Ohashi, Y. Kobuke, K. Kamada, K. Ohta, *J. Am. Chem. Soc.* **2003**, *125*, 13356–13357.
- [11] a) I. V. Sazanovich, A. Balakumar, K. Muthukumar, E. Hindin, C. Kirmaier, J. R. Diers, J. S. Lindsey, D. F. Bocian, D. Holten, *Inorg. Chem.* **2003**, *42*, 6616–6628; b) M. Speckbacher, L. Yu, J. S. Lindsey, *Inorg. Chem.* **2003**, *42*, 4322–4337; c) W. J. Youngblood, D. T. Gryko, R. K. Lammi, D. F. Bocian, D. Holten, J. S. Lindsey, *J. Org. Chem.* **2002**, *67*, 2111–2117; d) S. Prathapan, S. I. Yang, J. Seth, M. A. Miller, D. F. Bocian, D. Holten, J. S. Lindsey, *J. Phys. Chem. B* **2001**, *105*, 8237–8248; e) S. I. Yang, S. Prathapan, M. A. Miller, J. Seth, D. F. Bocian, J. S. Lindsey, D. Holten, *J. Phys. Chem. B* **2001**, *105*, 8249–8258.
- [12] W. D. Horrocks Jr, M. Albin in *Progress in Inorganic Chemistry* (Ed.: S. J. Lippard), John Wiley & Sons, New York, **1984**, vol. 31, pp. 1–104.
- [13] a) J. A. Teprovich Jr, E. Prasad, R. A. Flowers, *Angew. Chem.* **2007**, *119*, 1163–1166; *Angew. Chem. Int. Ed.* **2007**, *46*, 1145–1148; b) K. A. Gschneider Jr, L. Eyring, *Handbook on the Physics and Chemistry of Rare Earths*, North-Holland, Amsterdam, **1979**, vol. 15; c) P. Dorenbos, *J. Phys.: Condens. Matter* **2003**, *15*, 575–594.
- [14] a) H. He, X. Zhu, A. Hou, J. Guo, W. K. Wong, W. Y. Wong, K. F. Li, K. W. Cheah, *Dalton Trans.* **2004**, 4064–4073; b) H. S. He, Z. X. Zhao, W. K. Wong, K. F. Li, J. X. Meng, K. W. Cheah, *Dalton Trans.* **2003**, 980–986; c) W. K. Wong, A. Hou, J. Guo, H. He, L. Zhang, W. Y. Wong, K. F. Li, K. W. Cheah, F. Xue, T. C. W. Mak, *J. Chem. Soc. Dalton Trans.* **2001**, 3092–3098; d) W. K. Wong, L. L. Zhang, W. T. Wong, F. Xue, T. C. W. Mak, *J. Chem. Soc. Dalton Trans.* **1999**, 615–622.
- [15] D. Imbert, M. Cantuel, J.-C. G. Bünzli, G. Bernardinelli, C. Piguet, *J. Am. Chem. Soc.* **2003**, *125*, 15698–15699.
- [16] N. M. Shavaleev, L. P. Moorcraft, S. J. A. Pope, Z. R. Bell, S. Faulkner, M. D. Ward, *Chem. Commun.* **2003**, 1134–1135.
- [17] S. I. Klink, H. Keizer, F. C. J. M. van Veggel, *Angew. Chem.* **2000**, *112*, 4489–4491; *Angew. Chem. Int. Ed.* **2000**, *39*, 4319–4321.
- [18] S. I. Klink, L. Grave, D. N. Reinhoudt, F. C. J. M. van Veggel, M. H. Werts, F. A. J. Geurts, J. W. Hofstraat, *J. Phys. Chem. A* **2000**, *104*, 5457.
- [19] Z. R. Reeves, K. L. V. Mann, J. C. Jeffery, J. A. McCleverty, M. D. Ward, F. Barigelletti, N. Armaroli, *J. Chem. Soc. Dalton Trans.* **1999**, 349–356.
- [20] Y. Kawamura, Y. Wada, S. Yanagida, *Jpn. J. Appl. Phys.* **2001**, *40*, 350–356.
- [21] G. F. De Sá, O. L. Malta, C. de Mello Donegai, A. M. Simas, R. L. Longo, P. A. Santa-Cruz, E. F. da Silva Jr, *Coord. Chem. Rev.* **2000**, *196*, 165–195.
- [22] R. Reisfeld, C. K. Jorgensen, *Lasers and Excited States of Rare Earths*, Springer, Berlin, **1977**.
- [23] X. Zhu, PhD Thesis, Hong Kong Baptist University, **2006**.
- [24] M. H. V. Werts, J. W. Hofstraat, F. A. J. Geurts, J. W. Verhoeven, *Chem. Phys. Lett.* **1997**, *276*, 196–201.
- [25] a) H.-S. He, J.-P. Guo, Z.-X. Zhao, W. K. Wong, W. Y. Wong, W. K. Lo, K. F. Li, L. Luo, K. W. Cheah, *Eur. J. Inorg. Chem.* **2004**, 837–845; b) W. K. Wong, H. Liang, W. Y. Wong, Z. Cai, K. F. Li, K. W. Cheah, *New J. Chem.* **2002**, *26*, 275–278; c) W. K. Wong, A. Hou, J. Guo, H. He, L. Zhang, W. Y. Wong, K. F. Li, K. W. Cheah, F. Xue, T. C. W. Mak, *J. Chem. Soc. Dalton Trans.* **2001**, 3092–3098.
- [26] S. Faure, C. Stern, E. Espinosa, J. Douville, R. Guillard, P. D. Harvey, *Chem. Eur. J.* **2005**, *11*, 3469–3481.
- [27] R. L. Brookfield, H. Ellul, A. Harriman, G. Porter, *J. Chem. Soc. Faraday Trans. 2* **1986**, *82*, 219–233.
- [28] S. Kawata, H.-B. Sun, T. Tanaka, K. Takada, *Nature* **2001**, *412*, 697–698.
- [29] A. Karotki, M. Khurana, J. R. Lepock, B. C. Wilson, *Photochem. Photobiol.* **2006**, *82*, 443–452.
- [30] M. Calvete, G. Y. Yang, M. Hanack, *Synth. Met.* **2004**, *141*, 231–243.
- [31] M. Drobizhev, A. Karotki, M. Kruk, A. Rebane, *Chem. Phys. Lett.* **2002**, *355*, 175–182.
- [32] D. G. Mclean, R. L. Sutherland, M. C. Brant, D. M. Brandelik, *Opt. Lett.* **1993**, *18*, 858–860.
- [33] a) J. W. Perry, K. Mansour, I.-Y. S. Lee, X.-L. Wu, P. V. Bedworth, C.-T. Chen, D. Ng, S. Marder, P. Miles, *Science* **1996**, *273*, 1533–1536; b) J. W. Perry, K. Mansour, S. R. Marder, K. J. Perry, D. Alvarez Jr, I. Choong, *Opt. Lett.* **1994**, *19*, 625–627.
- [34] a) X. Zhong, Y. Feng, S.-L. Ong, J. Hu, W.-J. Ng, Z. Wang, *Chem. Commun.* **2003**, 1882–1883; b) A. Krivokapic, H. L. Anderson, G. Bourhill, R. Ives, S. Clark, K. J. McEwan, *Adv. Mater.* **2001**, *13*, 652–656; c) G. Y. Yang, S. G. Ang, L. L. Chng, Y. W. Lee, E. W.-P. Lau, K. S. Lai, H. G. Ang, *Chem. Eur. J.* **2003**, *9*, 900–904; d) S. Vagin, M. Barthel, D. Dini, M. Hanack, *Inorg. Chem.* **2003**, *42*, 2683–2694; e) R. B. Martin, H. Li, L. Gu, S. Kumar, C. M. Sanders, Y.-P. Sun, *Opt. Mater.* **2005**, *27*, 1340–1345; f) S. Fu, G. Zhou, X. Zhu, C. Ye, W. K. Wong, Z. Li, *Chem. Lett.* **2006**, *35*, 802–803.
- [35] M. Sheik-Bahae, A. A. Said, E. W. Van Stryland, *Opt. Lett.* **1989**, *14*, 955–957.
- [36] R. J. Angelici, *Reagents for Transition Metal Complex and Organometallic Syntheses*, vol. 28 (Inorganic Syntheses), 1st ed., John Wiley & Sons, New York, **1990**.
- [37] C. A. Parker, W. T. Rees, *Analyst (London)* **1960**, *85*, 587–600.
- [38] *SAINT, Reference manual*, Siemens Energy and Automation, Madison, WI, **1994–1996**.
- [39] G. M. Sheldrick, *SADABS, Empirical Absorption Correction Program*, University of Göttingen, Germany, **1997**.
- [40] G. M. Sheldrick, *SHELXTL™, Reference manual*, version 5.1, Siemens, Madison, WI, **1997**.

Received: March 19, 2007  
Published Online: June 5, 2007